# CMB polarization with the Bicep and Keck experiments

Michael Crumrine

February 26, 2017

## 1 Introduction

The modern study of cosmology began with Einstein's publication of the general theory of Relativity in 1915 [6] and the development of the Einstein field equations. In 1922 Friedmann[7] - assuming a homogeneous, isotropic universe - constructed a solution to Einstein's field equation that serve as the basis for the standard model of cosmology. In the 1930s, observations by Hubble [9] showing the expansion of the universe provided the first evidence of the big bang. In 1965 Penzias and Wilson[12] provided further evidence for a big bang origin with the discovery of the Cosmic Microwave Background. Further observations of the universe showed near complete flatness and uniformity on scales exceeding the particle horizon. Then in 1981 Guth[8] suggested that a brief period of exponential expansion now known as inflation could resolve these issues.

### 1.1 History of the CMB

The BICEP and Keck experiments observe the Cosmic Microwave Background (CMB) which originates from photons in the early universe. In the hot big bang, the early universe was an energetic plasma in which photons scattered continuously from free protons and electrons

which prevented propagation over large distances. As the universe expanded, the temperature of this plasma decreased adiabatically until the free electrons and protons could combine to form neutral Hydrogen. After this era of recombination about 380,000 years after the big bang, the photons decoupled from the plasma and began free streaming through the universe in the direction of their last scattering. We observe these photons as a 2D "surface of last scattering".

Results from COBE in 1992[4] showed the CMB to have a nearly isotropic temperature spectrum corresponding to a 2.73K blackbody with fluctuations on the order of 10 $\mu$K corresponding to density perturbations. The CMB photons carry additional information besides the temperature spectrum in the form of their polarization the first signs of which were detected by DASI[11] in 2002. This majority of the polarization signal comes from Thompson scattering in the inhomogeneous temperature field of the early universe. However, an inflationary epoch would produce its own polarization signal due to the generation of gravitational waves. The search for this inflationary gravitational wave (IGW) signal is the ongoing target for the Bicep and Keck program.

## 2 Anisotropies in the CMB

The near-uniform temperature spectrum of the CMB contains faint temperature anisotropies on the order of 1 part in $10^5$. These temperature anisotropies are largely due to - Gaussian distributed - density fluctuations at recombination. Although we cannot predict the locations or magnitudes of these fluctuations we can examine their statistical properties by decomposition with the spherical harmonics:

$$\delta T(\theta, \phi) = \sum_{m=-\ell}^{\ell} \sum_{\ell=0}^{\infty} a_{\ell m} Y_{\ell m}(\theta, \phi) \tag{1}$$

Although this decomposition is a powerful tool, the universe is isotropic only in a statis-

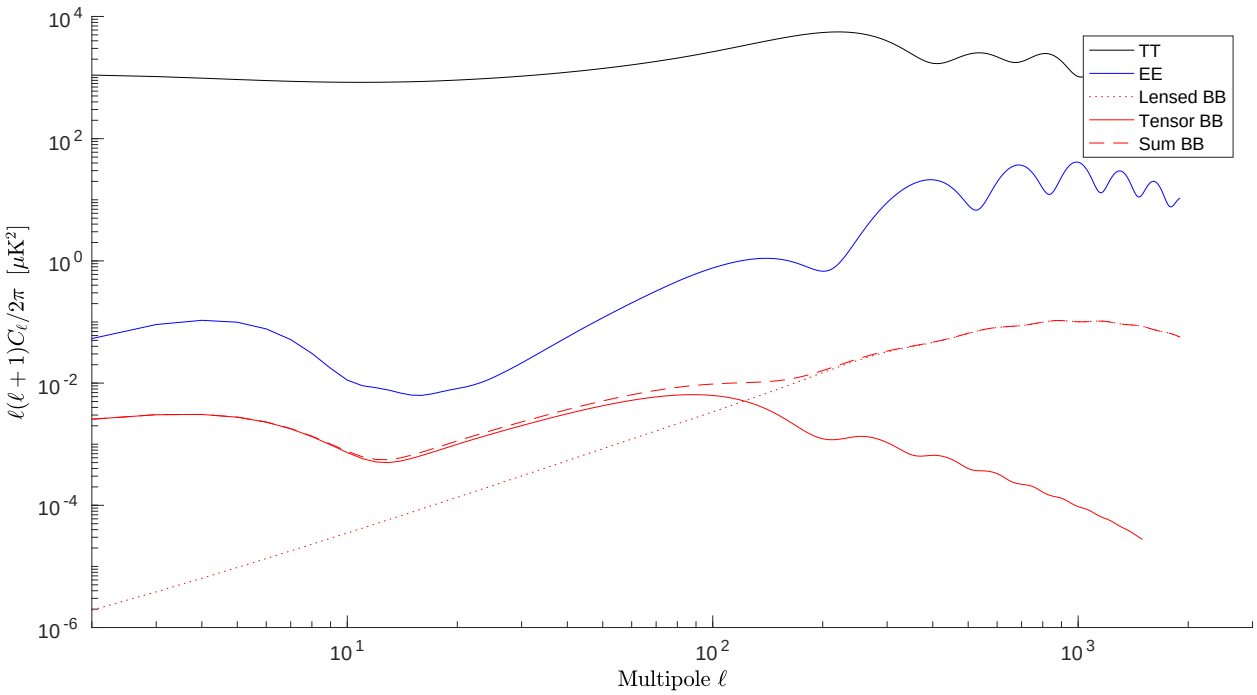


**Figure 1:** The CMB power spectrum of the ΛCDM standard model of cosmology as calculated by CAMB using parameters from Planck 2013. The temperature anisotropies (black) contain orders of magnitude more power than the E-mode (blue) and B-mode (red) polarization anisotropies. The BB spectrum is split into a lensing component (dotted) and a tensor component (solid) plotted at the $r = 0.1$ level.

tical sense and we therefore cannot predict any individual $a_{\ell m}$. We instead take an average over $m$ for a given $\ell$ to form the angular power spectrum:

$$C_\ell = \frac{1}{2\ell+1} \sum_{m=-\ell}^{\ell} \langle |a_{\ell m}|^2 \rangle \tag{2}$$

This angular power spectrum describes the relative power of features in the CMB according to their angular size with higher $\ell$ corresponding to smaller features. $\lambda$

## 2.1 Polarization Anisotropies

In addition to the temperature anisotropies that correspond to primordial density perturbations, CMB photons are partially polarized due to Thompson scattering in a non-uniform temperature field. This CMB polarization was predicted at the $\approx 10\%$ level by Bond et

al [5] and first detected by DASI in 2002 [11]. Polnarev [15] realized that an inflationary period would imprint an additional polarization signal on the CMB due to the production of gravitational waves.

This inflationary gravitational wave (IGW) signal is expected to be orders of magnitude fainter than the signal due to Thompson scattering and difficult to separate in the Stokes parameter space conventionally used in Electromagnetics when studying linearly polarized light. CMB polarization studies follow the procedures outlined in Kamionkowski et al [10] which separates the polarization signal into a gradient (E-mode) and curl (B-mode) component. The polarization signal produced by Thompson scattering occurs in the presence of a temperature quadrupole and follows the temperature gradients of the hot plasma at recombination while the IGW signal is not restricted in this way. Thompson scattering can therefore produce only E-modes while IGWs can produce both E and B modes. The signal produced by these two methods is characterised by the tensor to scalar ration $r$. Figure 1 shows the theoretical power spectra of CMB perturbations in the $\Lambda$CDM standard model of Cosmology with the addition of an $r = 0.1$ IGW B-mode signal.

# 3 The Bicep and Keck Program

The Bicep/Keck experiments are a staged series of small aperture ground based telescopes which aim to produce extremely deep degree-scale polarization maps of the CMB. Each generation of receiver builds on the experience gained from the previous generation while pushing deeper in sensitivity. This progression is shown in Figure 2.

Bicep1 was deployed to the south pole in 2006 and used 98 feedhorn coupled bolometers observing at 100GHz and 150GHz. Over three observing seasons the strategies developed for observation, calibration and systematics control proved the efficacy of small aperture refractors for CMB polarization studies and established the leading upper bounds on inflation

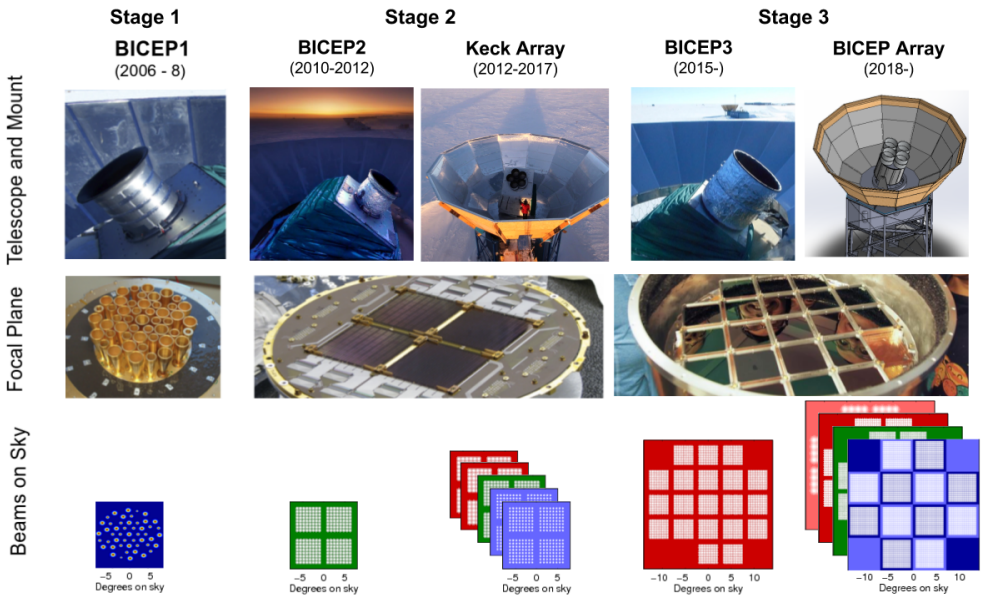


**Figure 2:** The progression of the Bicep/Keck program from Bicep1 to Bicep Array. The bottom row shows the beam patterns of the focal planes on the sky. With the exception of Bicep1 the focal plane colors correspond to band centers of: 35GHz - pink, 95GHz - red, 150GHz - green, 220 GHz - light blue, 270GHz - dark blue.

at $r < 0.70$ [1].

Building on the techniques developed with its predecessor, Bicep2 replaced Bicep1 in 2009. It exchanged feedhorn coupled bolometers for antenna-coupled transition edge sensor (TES) bolometer arrays developed at JPL which have been used in every subsequent telescope in the series. Concentrating its observing power at 150GHz, in March 2014 Bicep2 announced a detection of excess signal in its observing band consistent with an IGW signal of $r = 0.2$[2]. However, the interpretation of this excess as IGW signal relied heavily on models of polarized dust emission which had not been highly constrained at the time. Later that year new high frequency maps from the Planck experiment indicated that the dust models had underestimated polarized emission in the faintest sky regions [13]. A joint analysis with Planck and cross correlation between the Planck 353GHz and Bicep2 150GHz maps showed that a substantial part of the observed excess in Bicep2 was due to polarized dust emissions [3]. This joint analysis established a new upper limit of $r < 0.12$

Building on the observing power of Bicep2 the Keck Array deployed to the south pole in 2012 with five 150GHz receivers similar to Bicep2. These additional receivers confirmed the excess signal found with Bicep2 and contributed to the March 2014 results. In addition to extending the Bicep2 survey depth at 150GHz the Keck array has extended observations into three other observing bands at 95GHz, 220GHz and 270GHz. The extension into other frequencies harnesses the Bicep/Keck program's proven capability to make deep maps to further constrain galactic foregrounds and refine the models of polarized dust emission. The Keck array is in its final observing season with four receivers in the 220GHz band and one at 270GHz.

In the fall of 2014 Bicep3 was deployed at the south pole to run concurrently with the Keck array. Bicep3 vastly expands the design of the Bicep2 instrument with a focal plane containing 2500 detectors in the 95GHz band, almost 10x the 288 detectors of a Keck style 95GHz receiver. Bicep3 serves as our prototype instrument leading to the eventual replacement of the Keck array with Bicep array.

The Bicep array is a funded experiment which will replace the Keck Array for multifrequency observations. Using the more powerful Bicep3 style receivers, Bicep array will field three receivers centered at 35GHz, 95GHz, and 150GHz along with a dual band 220/270GHz receiver. The new 35GHz receiver will heavily constrain galactic synchrotron radiation past the upper limits set by WMAP's 23GHZ band while the increased sensitivity at higher frequencies will allow for better constraints on dust emissions at frequencies closer to our other bands than the Planck 353GHz data.

# 4 Multifrequency Observations

CMB polarization experiments must be able to separate polarized foreground signals from those imprinted on the CMB. Although these signals can be minimized by selection of ob-

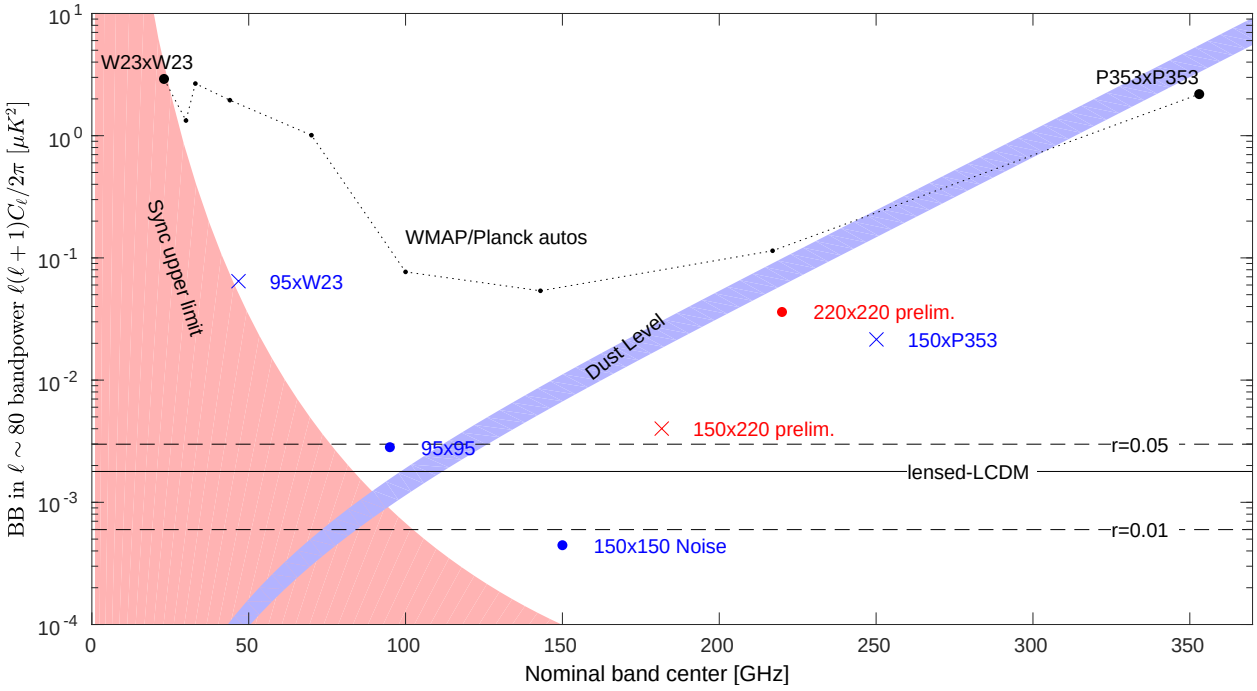


**Figure 3**

serving area their emissions must be constrained and accounted for. As shown by the 2014 joint analysis between Bicep2/Keck and Planck, constraints on these models have significant impact on the interpretation of any observed excess signal. By expanding observations into multiple frequencies, the Keck array has further constrained these dust emissions as well as emissions due to galactic synchrotron as shown in Figure 3.

## 4.1 Polarized Dust

Polarized emissions from galactic dust provide an excess BB signal on top of that expected from ΛCDM and gravitational lensing which (although low in power) are significant compared to the IGW signal. These emissions depend significantly on frequency, exhibiting a power law like dependence. As shown in Planck XXII [14] the spectral energy distribution of galactic dust can be described by a modified blackbody spectrum

$$I_d = A_d \nu^\beta B_\nu(T_d) \tag{3}$$

Where $A_d$ is an amplitude at some frequency and $\beta_d > 0$ is the spectral index of dust emission and $B(T)$ is the standard blackbody spectrum. In order to fully constrain the dust signal we must complement this intensity spectrum with a description of the dust's spatial behavior

$$D_\ell \propto \ell^\alpha \tag{4}$$

where $D_\ell = C_\ell \frac{\ell(\ell+1)}{2\pi}$. The parameters in these equations model the dust contribution to polarization signal in our field. As Equation 3 shows this signal is brighter at higher frequencies. We therefore use the Planck 353GHz maps to set these dust parameters and extrapolate to our observed frequencies. This necessarily means that any uncertainty contained in the high frequency observations is magnified due to the power law behavior.

Figure 3 shows the noise uncertainty and signal levels the $\ell = 80$ bandpower where the IGW signal is expected to peak. The low 150x150 noise allows us to detect excess signal with high significance. However, the high P353xP353 noise as compared to dust signal does not provide significant enough constraining power to separate dust signal from potential IGW signal in the 150GHz band. The 220x220 point shows preliminary numbers from our 2015 observing season in which the Keck array operated with two 220GHz receivers and provides similar constraining power to the Planck 353GHz data while being closer to our main observing bands. Two additional 220GHz receivers were added for the 2016 observing season and observations at 270GHz will begin in the current 2017 season. These observations will allow us to produce continually improving constraints on dust in our field.

## 4.2 Galactic Synchrotron

An upper limit for an additional foreground signal is shown in Figure 3. Rather than increasing in intensity at higher frequencies, polarized emissions from galactic synchrotron radiation are strongest at low frequencies. We model synchrotron emission intensity as

$$I_\nu = A_s \nu^{\beta_s} \tag{5}$$

where $\beta_s < 0$ describes the fall off in intensity with frequency and $A_s$ is the amplitude. The angular power spectrum of galactic synchrotron follows the same form as dust (Equation 4). The points shown in Figure 3 mark the upper limit of synchrotron emissions as the noise level of current observations in these bands is not sufficient for detection. Models of the contribution due to synchrotron do not predict significant contamination at frequencies upwards of 150GHz due to the strong frequency dependence. **Add in new BK15 plot with BK16 prelim points**

## 4.3 Bicep Array

The Bicep Array cryostat expands the Bicep 3 design to allow for observation at multiple frequencies.

-Widened 4K stage for extra baffling esp at 35GHZ -Same aperture size, throughput scales with num pixels -¿ frequency -Chart of pixel numbers and NETs per frequency across the receivers

# References


[1] D. Barkats et al. "Degree-scale Cosmic Microwave Background Polarization Measurements from Three Years of BICEP1 Data". In: *apj* 783, 67 (Mar. 2014), p. 67. DOI: 10.1088/0004-637X/783/2/67. arXiv: 1310.1422.

[2] BICEP2 Collaboration et al. "Detection of B-Mode Polarization at Degree Angular Scales by BICEP2". In: *Physical Review Letters* 112.24, 241101 (June 2014), p. 241101. DOI: 10.1103/PhysRevLett.112.241101. arXiv: 1403.3985.

[3] BICEP2/Keck and Planck Collaborations et al. "Joint Analysis of BICEP2/Keck Array and Planck Data". In: *Physical Review Letters* 114.10, 101301 (Mar. 2015), p. 101301. DOI: 10.1103/PhysRevLett.114.101301. arXiv: 1502.00612.

[4] N. W. Boggess et al. "The COBE mission - Its design and performance two years after launch". In: *apj* 397 (Oct. 1992), pp. 420–429. DOI: 10.1086/171797.

[5] J. R. Bond and G. Efstathiou. "Cosmic background radiation anisotropies in universes dominated by nonbaryonic dark matter". In: *apjl* 285 (Oct. 1984), pp. L45–L48. DOI: 10.1086/184362.

[6] A. Einstein. "Die Feldgleichungen der Gravitation". In: *Sitzungsberichte der Königlich Preußischen Akademie der Wissenschaften (Berlin), Seite 844-847.* (1915).

[7] A. Friedmann. "Über die Krümmung des Raumes". In: *Zeitschrift fur Physik* 10 (1922), pp. 377–386. DOI: 10.1007/BF01332580.

[8] A. H. Guth. "Inflationary universe: A possible solution to the horizon and flatness problems". In: *prd* 23 (Jan. 1981), pp. 347–356. DOI: 10.1103/PhysRevD.23.347.

[9] E. Hubble. "A Relation between Distance and Radial Velocity among Extra-Galactic Nebulae". In: *Proceedings of the National Academy of Science* 15 (Mar. 1929), pp. 168–173. DOI: 10.1073/pnas.15.3.168.

[10] M. Kamionkowski, A. Kosowsky, and A. Stebbins. "A Probe of Primordial Gravity Waves and Vorticity". In: *Physical Review Letters* 78 (Mar. 1997), pp. 2058–2061. DOI: 10.1103/PhysRevLett.78.2058. eprint: astro-ph/9609132.

[11] J. M. Kovac et al. "Detection of polarization in the cosmic microwave background using DASI". In: *nat* 420 (Dec. 2002), pp. 772–787. DOI: 10.1038/nature01269. eprint: astro-ph/0209478.

[12] A. A. Penzias and R. W. Wilson. "A Measurement of Excess Antenna Temperature at 4080 Mc/s." In: *apj* 142 (July 1965), pp. 419–421. DOI: 10.1086/148307.

[13] Planck Collaboration et al. "Planck intermediate results. XIX. An overview of the polarized thermal emission from Galactic dust". In: *aap* 576, A104 (Apr. 2015), A104. DOI: 10.1051/0004-6361/201424082. arXiv: 1405.0871.

[14] Planck Collaboration et al. "Planck intermediate results. XXII. Frequency dependence of thermal emission from Galactic dust in intensity and polarization". In: *aap* 576, A107 (Apr. 2015), A107. DOI: 10.1051/0004-6361/201424088. arXiv: 1405.0874.

[15] A. G. Polnarev. "Polarization and anisotropy induced in the microwave background by cosmological gravitational waves". In: *azh* 62 (Dec. 1985), pp. 1041–1052.